International Journal of Modern Physics C
Vol. 14, No. 6 (2003) 835–845

World Scientific
www.worldscientific.com

ACCELERATED LATTICE BGK METHOD FOR UNSTEADY SIMULATIONS THROUGH MACH NUMBER ANNEALING

A. M. ARTOLI*, A. G. HOEKSTRA†, and P. M. A. SLOOT‡
Section Computational Science, Faculty of Science, University of Amsterdam
Kruislaan 403, 1098 SJ Amsterdam, The Netherlands
*artoli@science.uva.nl
†alfons@science.uva.nl
‡sloot@science.uva.nl

Received 23 November 2002
Revised 23 December 2002

We present an adaptation of the lattice BGK method for fast convergence of simulations of laminar time-dependent flows. The technique is an extension to the recent accelerated procedures for steady flow computations. Being based on Mach number annealing, the present technique substantially improves the accuracy and computational efficiency of the standard lattice BGK method for such unsteady flows.

Keywords: Lattice BGK; unsteady flow; acceleration techniques; Mach number annealing.

1. Introduction

Due to its simple implementation, straightforward parallelism, easy grid generation, and its proven capability in simulations of multicomponent flows and complex geometry, the lattice Boltzmann method is now considered a mature computational fluid dynamics (CFD) flow solver. The method competes with traditional Navier–Stokes solvers by directly obtaining the pressure without a need to solve the Poisson equation and obtaining the stress tensor without using simulated velocity gradients.

In a previous article,[1] we have demonstrated the suitability and investigated the accuracy of the standard lattice-Boltzmann method with the simplified Bhatnagar, Gross and Krook[2] (BGK) collision operator in simulations of time-dependent fluid flows. We have also shown that the use of curved boundary conditions significantly enhances the accuracy as compared to the bounce-back on the links. However, the bounce-back rule is still the most popular boundary condition, for its simple implementation and easy adaptation to complex geometry. Unfortunately, the bounce-back rule produces large errors of first order behavior. In addition, simulations of time-dependent flows with the standard LBGK involve another major source of error: the compressibility errors. These two sources of error can be reduced

significantly by reducing the Mach number. This, unfortunately, blows up the computational time needed for the simulation to converge.[1,3]

A current computational interest for all CFD solvers is to optimize simulation parameters for a desired accuracy with minimum computational cost. Within the lattice Boltzmann community, many efforts have been reported towards this direction, mainly via implicit techniques,[4,5] local grid refinement[6,7] and scaling of the Reynolds number.[8] Most of these techniques are applied to steady flows and/or affect the uniformity of the Cartesian grid which has direct influence on parallelism in the computations. For unsteady flows, time evolution cannot be avoided and the method is computationally expensive, especially when the physical time scale is very small (which is a characteristic feature of dynamic complex systems). In this study, we extend these acceleration techniques to unsteady flows. The idea is based on stepwise reduction of the Mach number after the simulation converges with a higher Mach number. We call this process Mach number *annealing*. The paper is organized as follows. We give a short overview of LBGK, introduce the Mach number annealing technique, discuss benchmark simulations of unsteady systolic flow in a 3D tube, and end with concluding remarks.

2. The Lattice Boltzmann BGK Method

Since it was introduced[9–11] mainly to overcome the drawbacks of lattice-gas models, the lattice Boltzmann method has matured considerably over the years towards being a similar candidate to other computational fluid dynamics (CFD) solvers. The method is based on a discretized Boltzmann equation with a simplified collision operator via the single particle relaxation time approximation.[2] The LBGK scheme involves two steps[12,13]; streaming to the neighboring nodes and colliding with local node populations. Being represented by the probability f_i of a particle moving with a velocity $\mathbf{e}_i$ per unit time step δt, these populations are relaxed towards equilibrium during a collision process. The equilibrium distribution function

$$f_i^{(\mathrm{eq})} = w_i \rho \left(1 + \frac{3}{v^2}\mathbf{e}_i \cdot \mathbf{u} + \frac{9}{2v^4}(\mathbf{e}_i \cdot \mathbf{u})^2 - \frac{3}{2v^2}\mathbf{u} \cdot \mathbf{u}\right) \tag{1}$$

is a low-Mach number approximation to the expansion of the Maxwellian distribution. Here, w_i is a weighting factor, $v = \delta x/\delta t$ is the lattice speed, and δx and δt are the lattice spacing and the time step, respectively. Values for the weighting factor and the discrete velocities depend on the used LBGK model.[12] The well-known lattice BGK equation

$$f_i(\mathbf{x} + \mathbf{e}_i\delta_t, \mathbf{e}_i, t + \delta_t) - f_i(\mathbf{x}, \mathbf{e}_i, t) = -\frac{1}{\tau}[f_i(\mathbf{x}, \mathbf{e}_i, t) - f_i^{(0)}(\mathbf{x}, \mathbf{e}_i, t)] \tag{2}$$

can be obtained by discretizing the evolution equation of the distribution functions in the velocity space using a finite set of velocities $\mathbf{e}_i$. In this equation, τ is the dimensionless relaxation time. By Taylor expansion of the LBGK equation up to

$O(\delta t^2)$ and application of the multiscale Chapman–Enskog technique[12] through expansion of f_i about $f_i^{(0)}$, the Navier–Stokes equations and the momentum flux tensor up-to second order in the Knudsen number can be obtained. The hydrodynamic density ρ and the macroscopic velocity $\mathbf{u}$ are determined in terms of the particle distribution functions from $\rho = \sum_i f_i = \sum_i f_i^{(\mathrm{eq})}$ and $\rho\mathbf{u} = \sum_i \mathbf{e}_i f_i = \sum_i \mathbf{e}_i f_i^{(\mathrm{eq})}$. The pressure is given by $p = \rho c_s^2$ and the kinematic viscosity is $\nu = c_s^2 \delta t(\tau - (1/2))$, where c_s is the speed of sound. This LBGK model works pretty well as long as the Mach number M_a is low ($M_a^2 \ll 1$) and the density fluctuations are small. However, modeling unsteady flows involves higher density fluctuations, since the density and the unsteady pressure are tied up together through the ideal gas equation of state. The compressibility errors at high Mach numbers are also expected. Although there exists a number of incompressible versions of LBGK,[14] they have not been formulated and tested in three dimensions and are not yet popular. A number of generalized lattice Boltzmann equations are recently gaining more attention.[15] They provide more stable and accurate solutions, but at relatively higher computational cost. In this paper, we have applied the widely used quasi-incompressible D3Q19 model, which has three types of particles on each node; a rest particle, six particles moving along x, y, and z principal directions with speeds $|\mathbf{e}_i| = 1$, and 12 particles along the diagonals with speeds $|\mathbf{e}_i| = \sqrt{2}$.

3. Mach Number Annealing

The Mach number is defined as the ratio between the speed U of an object to the speed of sound c_s,

$$M_a = \frac{U}{c_s}\,. \tag{3}$$

Low-speed fluids ($M_a \ll 1$) can be considered as incompressible. As the Mach number approaches unity, compressibility effects need to be considered. The lattice BGK scheme involves a low-Mach number expansion of the Maxwell equilibrium distribution function and therefore, it introduces compressibility errors at relatively high Mach numbers.

In addition to the kinematic viscosity ν, the diameter D and the velocity U which define the Reynolds number as $\mathrm{Re} = UD/\nu$, a nonsteady flow is characterized by a characteristic time interval, included in the Womersley parameter $\alpha = (D/2)\sqrt{\omega/\nu}$ or the Strouhal number, $\mathrm{St} = Df/U = 2\alpha^2/\pi\,\mathrm{Re}$ where $\omega = 2\pi f = 2\pi/T$ is the angular frequency with f being a typical frequency and T the associated period of oscillation. An additional constraint comes from the fact that the accuracy of LBGK reduces with increasing Mach number, especially for unsteady flows. The flow problem is completely defined by the geometry and these dimensionless numbers take certain constant values. Now, in order to simulate at low-Mach number, we must decrease the velocity U and consequently decrease the viscosity ν to produce the same Reynolds number. However, since the Womersley and the Strouhal

numbers are dependent on the viscosity and the velocity, the frequency must also be reduced. Explained in formulas, the velocity U is given by

$$U = \frac{\mathrm{Re}\,\nu}{D} = \frac{Df}{\mathrm{St}} = M_a c_s \tag{4}$$

from which

$$M_a = \frac{\mathrm{Re}\,\nu}{c_s D}\,, \tag{5}$$

and

$$\mathrm{Re} = \frac{D^2 f}{\nu\,\mathrm{St}}\,. \tag{6}$$

From these relations, we recognize that the Mach number M_a and the kinematic viscosity ν are directly proportional to the frequency of oscillation through

$$M_a = \frac{fD}{\mathrm{St}\,c_s}\,, \tag{7}$$

$$\nu = \frac{fD^2}{\mathrm{St}\,\mathrm{Re}}\,, \tag{8}$$

and

$$\nu = \frac{\pi D^2 f}{2\alpha^2}\,. \tag{9}$$

Equation (7) implies that the frequency domain has to be reduced in order to have a low Mach number. This results in a considerable delay in the convergence behavior. Equation (8) shows that decreasing the frequency unfortunately results in pushing the simulation towards the instability region of LBGK. Equation (9) tells us that, for highly dynamic simulations (high α), we need to consider both low frequency and viscosity. These constraints end up with a computationally expensive slowly time evolving simulation. This poses a high demand on a prospective acceleration method.

An annealing process to accelerate the lattice Boltzmann method was first reported by Bernaschi *et al.*[8] It allows fast convergence by combining viscosity annealing with powerful linear iterative solvers for computing the inverse Liouville operator.

Different from those for steady flows, time-dependent LBGK simulation parameters are not easy to control within a running simulation since, among others, new physical and hydrodynamic constraints need to be satisfied. The flow is now characterized by the Womersley number, the Reynolds number, and the Strouhal number, as discussed above. These parameters need to be fixed during annealing since the dynamics of the flow is highly time-dependent. We apply the same idea for unsteady flows, but anneal the Mach number instead of the Reynolds number on a strictly fixed spatial grid. We assume that the Mach number is to be annealed n times and recall n as the annealing factor. In order to do that

$$n = \frac{M_a}{M_a'} = \frac{U}{U'} = \frac{f}{f'} = \frac{\nu}{\nu'}\,, \tag{10}$$

which implies that all the velocity (in terms of the driving force), the frequency of oscillation and the viscosity are to be reduced n times. This annealing strategy can be direct (one level annealing) or multilevel. In the direct annealing strategy, after the simulation converges with a higher Mach number, the viscosity, the frequency and the driving force are reduced n times in a single step and the simulation converges to the final solution. The multilevel annealing strategy involves gradual reduction of these parameters towards n, depending on the stability and tolerance constraints. In other words, there are different ways to decide when to start the annealing. Examples of both direct and multilevel annealing methods are discussed in the next section.

4. Simulations

We consider time-dependent systolic flow in a rigid tube of diameter $D = 63$ lattice units as a benchmark for our simulations. The first eight harmonics of a pressure pulse, measured at the entrance of the human abdominal aorta, are used to apply an inlet condition for the tube. We have selected this complex time series for the sake of generality. For the outlets, constant density is applied. The velocity and the unknown distributions are computed from the density. For the walls, the bounce-back on the links is used. For all simulations the Womersley number is kept constant at $\alpha = 16$ and the average Reynolds number is $\mathrm{Re} = 270$. The simulation starts at average $M_a = 0.5$ ($T = 360$ and $\nu = 0.068$) and waits until the system builds up its knowledge about the pulsatility and nonlinear behavior and converges after about 40 complete periods. The obtained simulation results are compared with the real part of the analytical Womersley solution

$$u(y,t) = \sum_{m=1}^{8} \left[-\frac{A_m}{\rho\omega_m} e^{-i\omega_m t} \left(1 - \frac{J_0[y\sqrt{b_m}]}{J_0[R\sqrt{b_m}]} \right) \right] , \tag{11}$$

where A_m is the amplitude of the pressure gradient, $R = D/2$ is the radius of the tube, J_0 is the zeroth order Bessel function of the first type and $b_m = -i\omega_m/\nu$ with $\omega_m = m\omega_1$ and $\omega_1 = 2\pi/T$ for the mth Fourier harmonics. The average error at $M_a = 0.5$ is 15%, originating from both compressibility effects and wall boundary conditions. Next, we reduce the Mach number to obtain good agreement with the analytical solution. We have previously studied the effect of reducing the Mach number on the accuracy for this benchmark.[16] Figure 1 shows sample simulation results for three different time frames after reducing the Mach number to $M_a = 0.1$. The new simulation parameters are computed from Eq. (10) after substituting $n = 5$ and including the initial simulation parameters. The average error is reduced to less than 1%. However, since the period increases five times, the computational time increases with the same factor. The aim of Mach number annealing is to accelerate convergence to equilibrium by reducing the percentage tolerance in mass and momentum, computed by comparing similar points for each

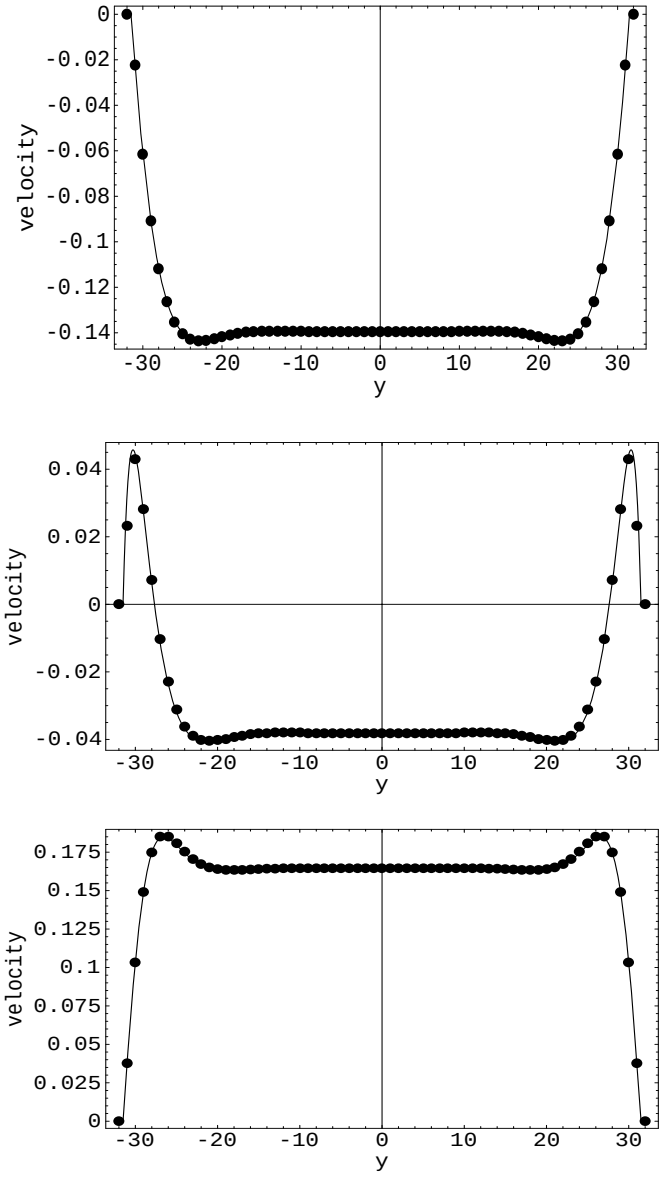

(a)

Fig. 1. The obtained (•) (a) velocity profiles and (b) shear stress in lattice units during (c) the systolic cycle, compared to the analytical Womersley solution (——) for the 3D tube benchmark. The dots in (c) indicate times at which the profiles are shown. For this simulation $\alpha = 16$, $\mathrm{Re} = 270$, and $M_a = 0.1$.

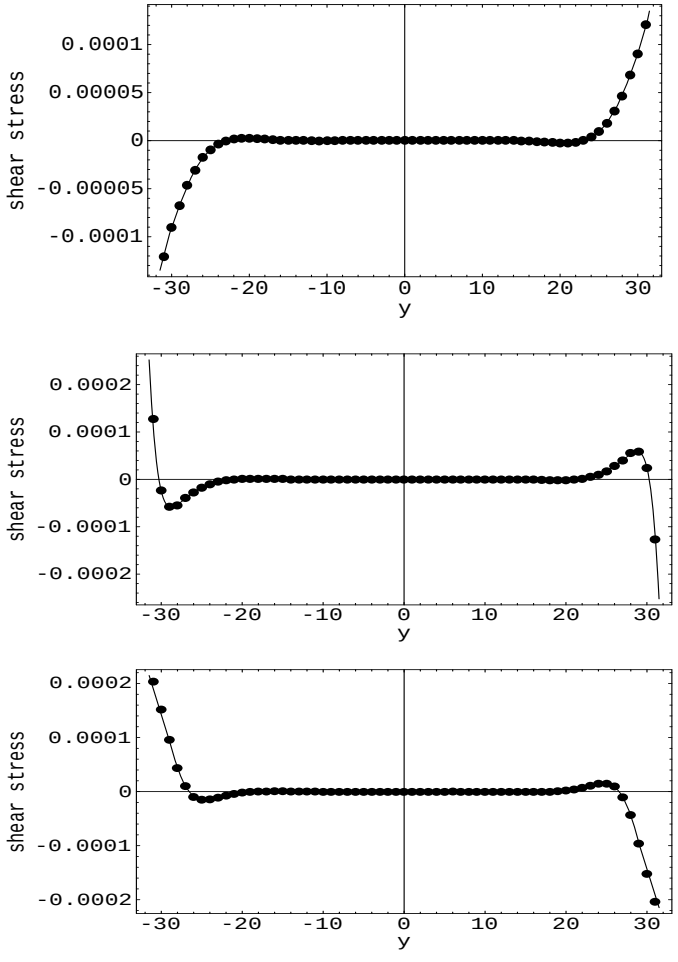

(b)

Fig. 1 (*Continued*)

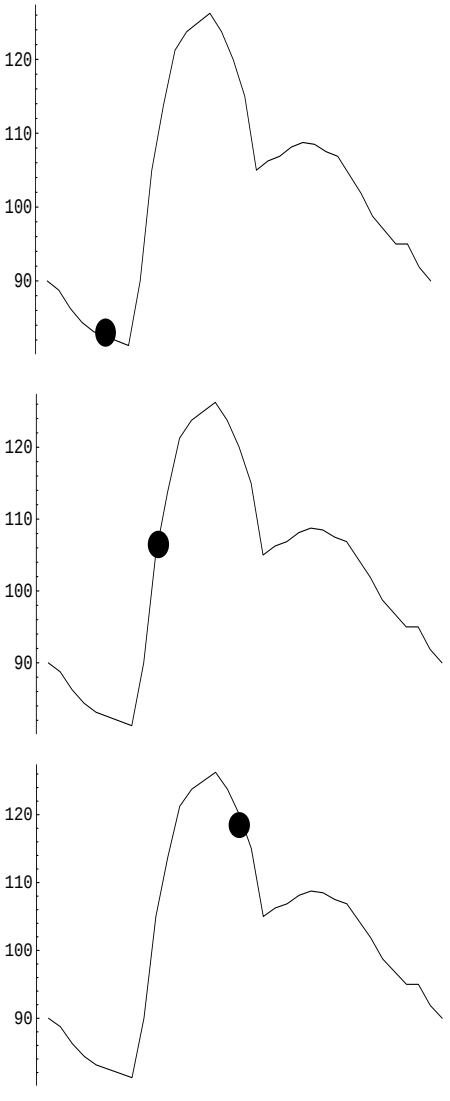

(c)

Fig. 1 (*Continued*)

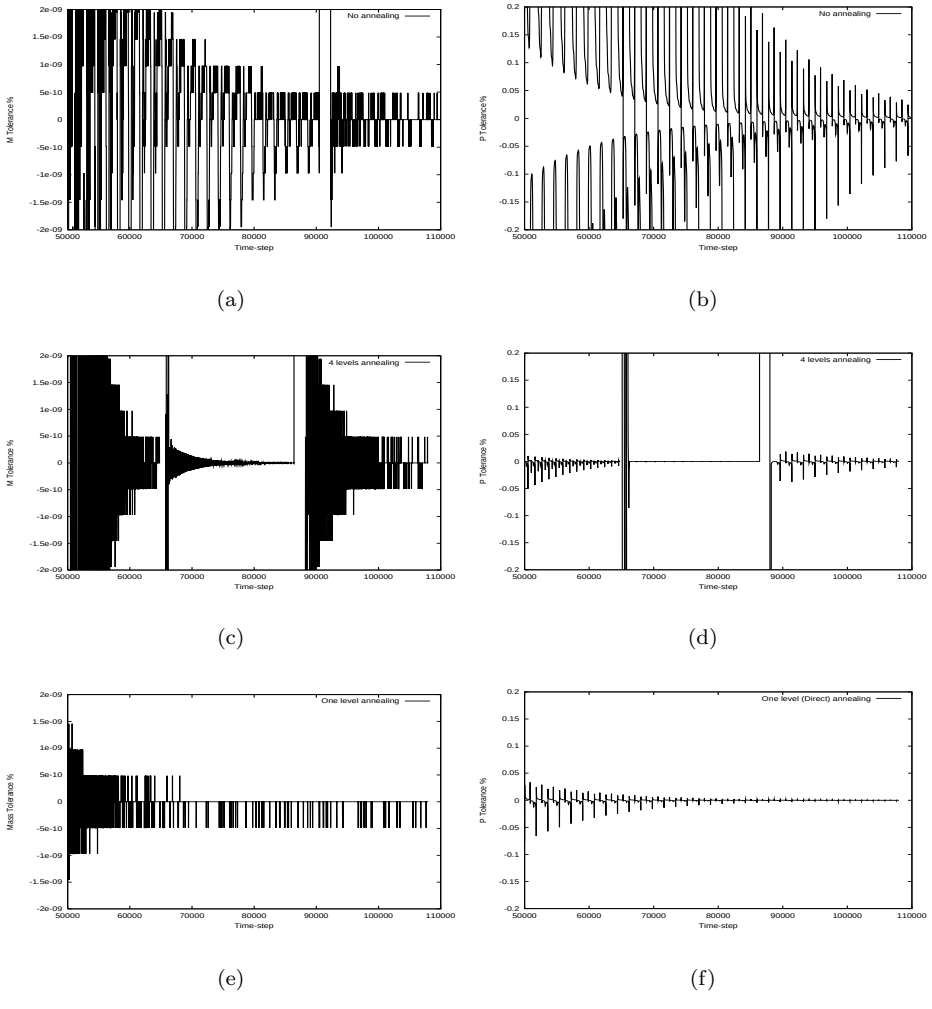

Fig. 2. Comparison in mass (left) and momentum (right) tolerance as a function of number of time-steps, between nonannealed (upper row), four levels annealed (middle row) and directly annealed (bottom) simulations. The Mach number is reduced five times in the annealed simulations (from 0.5 to 0.1).

two successive periods. The mass tolerance is defined as

$$M \text{ tolerance}\,\% = \frac{M(t) - M(t-T)}{M(t-T)} * 100 \tag{12}$$

and the momentum tolerance is defined accordingly.

In typical simulations, we accept convergence below 0.1% for the momentum. We have performed three simulation sets for the systolic tube flow benchmark: One without annealing with the lowest desired Mach number, having $T = 1800$ and $\nu = 0.01353$. The pressure gradient is scaled to obtain a Mach number of 0.1.

Figures 2(a) and 2(b) show the relaxation of tolerance in mass and momentum from which we see that it takes quite a long time to damp out the initial oscillations in tolerance (more than 72 000 time-steps). The second set of simulations is conducted using four levels of annealing by reducing the Mach number after each 60 periods of the basic simulation. In detail, the Mach number is reduced to 0.4, 0.3, 0.2 and finally 0.1 directly after 60, 120, 180 and 240 complete periods of the basic simulation, respectively. The results are shown in Figs. 2(c) and 2(d), from which we notice that the mass and more strongly the momentum converge much faster with the annealing process. The momentum tolerance is usually several orders of magnitudes higher than that for the mass, and hence, has more influence on the accuracy of the flow fields.

The third set shows a one-step annealing in which the simulation parameters are directly tuned to the final Mach number ($M_a = 0.1$) after convergence of the basic simulation in which $T = 360$ and $M_a = 0.5$. The direct annealing strategy significantly accelerates the relaxation towards equilibrium (see Figs. 2(e) and 2(f)), since it significantly reduces compressibility errors earlier than the multilevel annealing process. For the nonannealed case, it takes a long time for the momentum to relax with a tolerance similar to the directly annealed simulations. In terms of numbers, the direct annealing strategy is at least three times faster for a five times annealed Mach number. The gain in computational time is higher if the ratio between the two Mach numbers is larger, since the order in the tolerance seems to depend only on the tolerance of the initial simulations rather than the annealing factor.

The short-living spikes in Fig. 2 may be attributed to two reasons. First, since the systolic cycle is composed of many harmonic terms, values of point mass and momentum do not simultaneously converge. Compressibility errors at high velocities are also large. This explains why the spikes disappear with direct annealing, since the Mach number is significantly reduced.

5. Conclusions

In this paper we have presented a numerical technique to accelerate laminar time-dependent LBGK simulations through annealing of the Mach number during simulations, either directly or in a multilevel strategy. In both cases, the simulation is performed on a fixed grid and the viscosity, the Mach number, and the frequency are annealed by the same annealing factor. Considerable gain in computational time compared to that for the nonannealed standard LBGK simulations is observed. We have shown that direct annealing of the Mach number is faster than the multilevel one. Since it works on the same grid, the Mach number annealing technique does not affect the parallelism of the uniform LBE Cartesian grid. Our current research concentrates on the optimization of different annealing strategies of the Mach number for best acceleration.

Acknowledgment

This work is partially funded by the Steunfonds Soedanese Studenten, Leiden, The Netherlands.

References

1. A. M. Artoli, A. G. Hoekstra, and P. M. A. Sloot, *Int. J. Mod. Phys. C* **13**, 1119 (2002).
2. P. L. Bhatnagar, E. P. Gross, and M. Krook, *Phys. Rev. A* **94**, 511 (1954).
3. R. S. Maier, R. S. Bernard, and D. W. Grunau, *Phys. Fluids* **8**, 1788 (1996).
4. R. Verberg and A. Ladd, *Phys. Rev. E* **60**, 3366 (1999).
5. J. Tölke, M. Krafczyk, M. Schulz, E. Rank, and R. Berrios, *Int. J. Mod. Phys. C* **9**, 1143 (1998).
6. O. Filippova and D. Hänel, *J. Comput. Phys.* **147**, 219 (1998).
7. D. Z. Yu, R. W. Mei, and W. Shyy, *Int. J. Numer. Meth. Fluids* **39**, 99 (2002).
8. M. Bernaschi, S. Succi, H. D. Chen, and R. Y. Zhang, *Int. J. Mod. Phys. C* **13**, 675 (2002).
9. S. Succi, E. Foti, and F. Higuera, *Europhys. Lett.* **10**, 433 (1989); F. Higuera, S. Succi, and R. Benzi, *Europhys. Lett.* **9**, 345 (1989); R. Benzi, S. Succi, and M. Vergassola, *Phys. Rep.* **222**, 145 (1992).
10. H. Chen, S. Chen, and W. H. Matthaeus, *Phys. Rev. A* **45**, 5339 (1992).
11. G. McNamara and G. Zanetti, *Phys. Rev. Lett.* **61**, 2332 (1988).
12. S. Succi, *The Lattice Boltzmann Equation for Fluid Dynamics and Beyond* (Oxford University Press, 2001); B. Chopard and M. Droz, *Cellular Automata Modeling of Physical Systems* (Cambridge University Press, 1998).
13. X. He and L. S. Luo, *Phys. Rev. E* **56**, 6811 (1997).
14. X. He and L. Luo, *J. Stat. Phys.* **88**, 927 (1997); Q. Zou, S. Hou, S. Chen, and G. D. Doolen, *J. Stat. Phys.* **81**, 35 (1995); Z. L. Guo, B. C. Shi, and N. C. Wang, *J. Comput. Phys.* **165**, 288 (2000).
15. D. d'Humières, *Rarefied Gas Dynamics: Theory and Simulations. Prog. Aeronaut. Astronaut.* **159**, 450 (1992); D. d'Humières, I. Ginzburg, M. Krafczyk, P. Lallemand, and L. S. Luo, *Phil. Trans. R. Soc. Lond. A* **360**, 437 (2002).
16. A. M. Artoli, A. G. Hoekstra, and P. M. A. Sloot, submitted (2002).